Three-dimensional flow near the flapping wings

D. Kolomenskiy,[1, 2, *] H. K. Moffatt,[2] M. Farge,[3] and K. Schneider[1, 4]

[1]*M2P2–CNRS, Universités d'Aix-Marseille, Marseille, France*
[2]*DAMTP, University of Cambridge, U.K.*
[3]*LMD–CNRS, Ecole Normale Supérieure, Paris, France*
[4]*CMI, Université de Provence, Marseille, France*

One of the major hypotheses underlying many aerodynamic theories states that the flow near the wings can be sufficiently well described within the two-dimensional approximation. This viewpoint is classical and very appealing since it greatly simplifies the modelling. The two-dimensional approximation is well justified for propellers, but experiments with insects showed new and important three-dimensional effects [1]. Obviously, they are also relevant to insect-like flying robots.

The three-dimensional character of the flow strongly influences the dynamics of the vortex shedding. Even though the wings operate at large angles of attack, the leading-edge vortices persist over the upper surfaces and increase the lift. This feature makes a striking contrast to the periodic vortex shedding that occurs in the two-dimensional motion. This 'stable' behaviour of the leading-edge vortices is accompanied by a strong flow in the spanwise direction [2]. In the present work we explore this flow using numerical simulations and propose a very simple, but elucidating, potential flow model.

The numerical simulations are performed using the method described in [3, 4]. The wings rotate with respect to hinges situated at their roots. Initially the wings touch with their upper surfaces. They start to rotate first about the trailing edges, the angle α increases up to $45°$. Then they rotate about the vertical. The Reynolds number is $Re = 128$.

Figure 1 depicts the absolute value of the vorticity at three time instants. At time $t = 1.2$, very strong leading-edge vortices are seen. Equally strong vortices are generated at the wing tips. This
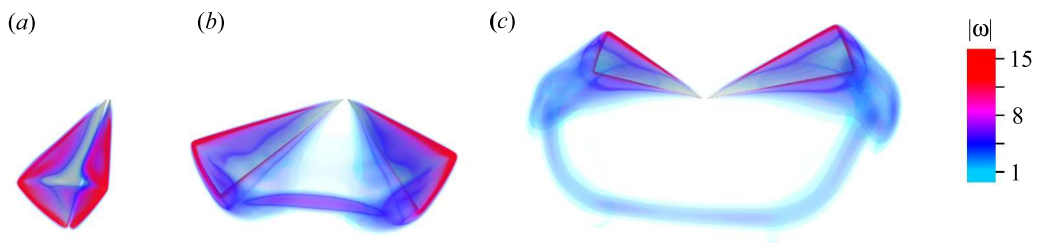

Figure 1: Vorticity magnitude at time instants $t = 1.2$ (*a*), 3.2 (*b*) and 7.2 (*c*).

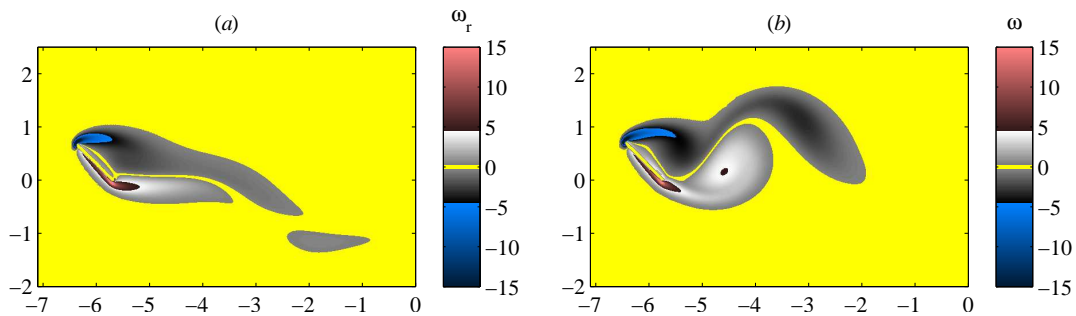* Electronic address: dkolom@L3m.univ-mrs.fr

Figure 2: Radial component of the three-dimensional vorticity probed on a cylinder surface $r = 0.75R$ (a) and the result of the two-dimensional numerical simulation (b). Time $t = 7.2$. R is the wing length.
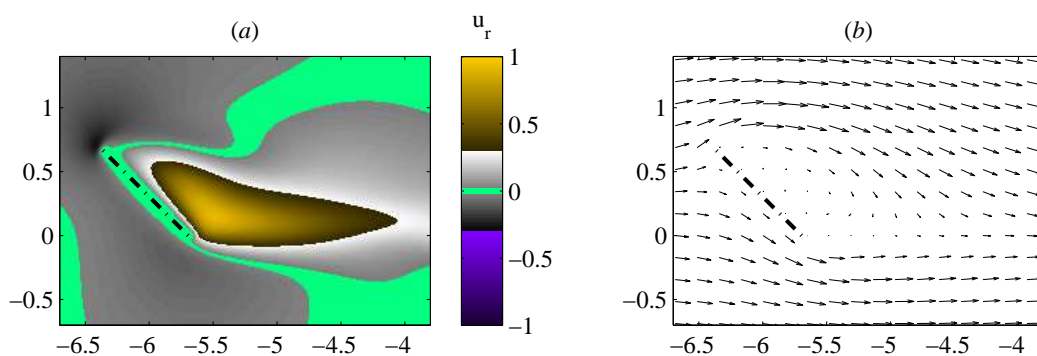

Figure 3: Radial (a) and tangential (b) components of the velocity in the cross-section $r = 0.75R$ at time $t = 7.2$.

vorticity results from the air flow into the opening space between the wings past its sharp edges. Also note a vortex which reconnects the wing ends. It forms a horseshoe shape at later times, $t = 3.2$ and 7.2. At $t = 7.2$ the vortices shed from the wing ends resemble hairpins typical for flows past three-dimensional bluff bodies like spheres or disks.

It is straightforward to compare these results with those predicted within the two-dimensional approximation. In figure 2, a cylindrical section of the three-dimensional radial vorticity field (a) is compared with the two-dimensional result (b). The dynamics of the free vortices in the two cases is different. In the two-dimensional simulation, the leading- and the trailing-edge vortices grow in strength until they are subsequently shed, and the process would repeat periodically if the wings continued to move further. The three-dimensional vortices are less intense, but they remain attached and their strength remains constant in time. The near flow field of a wing is approximately steady in a moving reference frame.

The radial velocity is displayed in figure 3(a). The strong spanwise flow from the root to the tip occupies a large domain behind the wing, but this is not where the vorticity is strong (*cf.* figure 2a). The vorticity is the strongest near the sharp edges, where, surprisingly, the spanwise flow is in the opposite direction, from the tip to the root. These features can also be observed in real insect configurations [5].

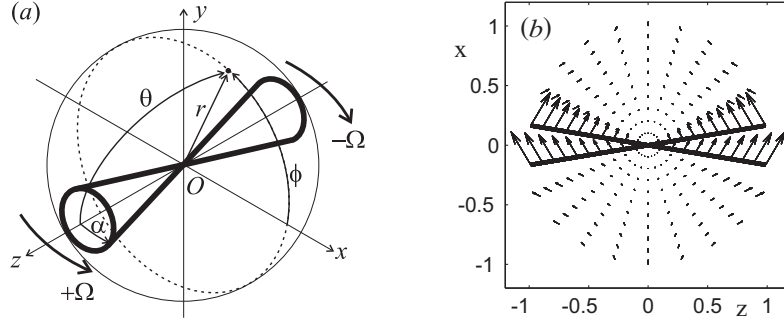The reason for the strong spanwise flow from root to tip behind the upper surface is evident from the

Figure 4: Schematic of two counter-rotating cones (*a*) and the potential velocity in the horizontal plane (*b*).

velocity field relative to the wing, shown in figure 3(*b*). It reveals a recirculation bubble, and centrifugal forces acting on it generate the spanwise flow.

The opposite flow in front of the wings is a consequence of the incompressibility. Let us consider the potential flow with the potential

$$\Phi = \frac{\Omega r^2 Q_2^1(\cos\theta)\cos\phi}{\mathrm{d}Q_2^1(\cos\alpha)/\mathrm{d}\alpha}, \quad \text{where} \quad Q_2^1(\cos\theta) = -\frac{3}{2}\cos\theta\sin\theta\ln\frac{1+\cos\theta}{1-\cos\theta} + 2\sin\theta - \frac{\cos^2\theta}{\sin\theta}, \quad (1)$$

This flow corresponds to two cones of an infinite length which rotate in opposite directions, as shown in figure 4(*a*). Ω is the angular velocity, α is the angle at the vertex of the cone, r, θ, ϕ are the polar coordinates. Figure 4(*b*) displays the velocity in the horizontal plane. Its radial component is outwards behind the cones and inwards in front of them, in agreement with the numerical simulation. Its peak value depends on the angle α at the vertex of the cone, almost linearly when $\alpha < \pi/10$,

$$u_r \approx -2\alpha\Omega r\cos\phi \quad \text{on} \quad \theta = \alpha. \tag{2}$$

A similar dependence may be expected in the more complex case of two flat plates in a real fluid.

[1] A. P. Willmott, C. P. Ellington and A. L. R. Thomas. 1996. Flow visualization and unsteady aerodynamics in the flight of the hawkmoth, Manduca sexta. *Phil. Trans. R. Soc. Lond. B*, **352**, 303-316.

[2] T. Maxworthy, 1979. Experiments on the Weis-Fogh mechanism of lift generation by insects in hovering flight. Part 1. Dynamics of the 'fling'. *J. Fluid Mech.*, **93**(1), 47-63.

[3] D. Kolomenskiy and K. Schneider, 2009. A Fourier spectral method for the Navier–Stokes equations with volume penalization for moving solid obstacles. *J. Comput. Phys.*, **228**, 5687-5709.

[4] D. Kolomenskiy, H. K. Moffatt, M. Farge and K. Schneider, 2011. The Lighthill–Weis-Fogh clap-fling-sweep mechanism revisited. *J. Fluid Mech.*, accepted for publication.

[5] H. Aono, F. Liang and H. Liu, 2008. Near- and far-field aerodynamics in insect hovering flight: an integrated computational study. *J. Exp. Biol.*, **211**, 239-257.